PCCP

Accepted Manuscript

ROYAL SOCIETY OF CHEMISTRY

www.rsc.org/pccp

Journal Name

COMMUNICATION

A Cocatalyst-Free Eosin Y-Sensitized P-type Co_3O_4 Quantum Dots for Highly Efficient and Stable Visible-Light-Driven Water Reduction and Hydrogen Production†

Received 00th January 20xx,
Accepted 00th January 20xx

DOI: 10.1039/x0xx00000x

www.rsc.org/

Ning Zhang,[a] Jinwen Shi,[a] Fujun Niu,[a] Jian Wang[a] and Liejin Guo[*a]

Owing to the effect of energy band bending, p-type Co_3O_4 quantum dots sensitized by eosin Y performed high and stable photocatalytic activity (~13440 μmol h^{-1} g^{-1}_{cat}) for water reduction and hydrogen production under visible-light irradiation without any cocatalyst.

Dye-sensitized semiconductor (DSS) system for photocatalytic water reduction and hydrogen production is considered as one of the most promising routes for making efficient use of solar light to produce clean energy.[1-4] In a typical DSS system, electrons are excited by light from dye and then transfer to the conduction band (CB) of semiconductor for reduction reaction. In order to reduce the overpotential of hydrogen evolution and improve reaction efficiency, cocatalysts are usually loaded on semiconductor catalysts.[5-7] However, until now, the large-scale use of cocatalysts are entirely unrealistic, because most paths for loading cocatalysts are of unacceptable high cost.

In this work, we reported a novel DSS system which performed high photocatalytic efficiency without any cocatalysts loading. Significantly, our system can keep stable photocatalytic activity for more than 35 hours. In this system, p-type Co_3O_4 quantum dots (Co_3O_4 QDs), which showed capability of splitting pure water under visible-light irradiation as we reported in the previous paper,[8] were used as catalyst, Eosin Y (EY) was used as dye and triethanolamine (TEOA) was used as sacrificial agent. Co_3O_4 QDs was prepared by the method according to ref[8], and the process of EY sensitization was described in ESI, finally a EY-sensitized Co_3O_4 QDs solution was obtained. To distinguish samples, original Co_3O_4 QDs was designed as Co_3O_4 QDs, and EY-sensitized Co_3O_4 QDs was designed as Co_3O_4 QDs/EY.

To explore the effect of EY sensitization on Co_3O_4 QDs, Co_3O_4 QDs/EY was separated from solution, washed with deionized water and then dried at 80°C in vacuum. Powder X-ray diffraction (PXRD) patterns (see Fig. S2, ESI†) reveals that the crystal phase of Co_3O_4 QDs is not changed after EY sensitization and are also in cubic phase (JCPDS Card No. 00-001-1152). Compared with Co_3O_4 QDs, a few diffraction peaks emerge at 2θ value below 30° in Co_3O_4 QDs/EY, which is probably due to EY adsorption. Survey-scan X-ray photoelectron spectroscopy (XPS) (see Fig. S3a, ESI†) proves that Co, O and C elements can be found in both Co_3O_4 QDs and Co_3O_4 QDs/EY. Different from Co_3O_4 QDs, satellite peak of C and feature peaks of Br 2p can be observed in the XPS spectrum of Co_3O_4 QDs/EY, which indicates EY existing on the surface of Co_3O_4 QDs. High-resolution XPS spectra of Co 2p (see Fig. S3b, ESI†) announce that peaks at 779.0, 780.5, 794.4, 795.8, 789.5, and 802.4 eV correspond to Co^{2+} ($2p_{1/2}$), Co^{3+} ($2p_{1/2}$), Co^{2+} ($2p_{3/2}$), Co^{3+} ($2p_{3/2}$), shake-up satellites of Co^{2+} ($2p_{1/2}$) and Co^{2+} ($2p_{3/2}$), respectively,[8,9] and the calculated area ratio of Co^{3+} ($2p_{3/2}$) to Co^{2+} ($2p_{3/2}$) for both samples approximates to 2. Thus it is deduced that both Co_3O_4 QDs and Co_3O_4 QDs/EY are in the chemical form of $Co^{2+}(Co^{3+})_2O_4$. Transmission electron microscopy(TEM) image (see Fig. S4a, ESI†) indicates that the morphology of Co_3O_4 QDs is agglomerated nanocrystals in size of 3-4 nm, which agrees with previous report.[8] The morphology of Co_3O_4 QDs/EY is similar to Co_3O_4 QDs (see Fig. S4b, ESI†), which implies that EY sensitization cannot affect the morphology of Co_3O_4 QDs.

The Fourier transform infrared spectra (FTIR) of Co_3O_4 QDs/EY and Co_3O_4 QDs are shown in Fig. S5 (ESI†). The feature peaks centering at 559 cm^{-1} and 659 cm^{-1}, assigned to Co–O stretching and Co–OH vibrations,[10] are observed in FTIR spectra of both Co_3O_4 QDs/EY and Co_3O_4 QDs, which confirm that the two samples contain cobalt oxide. It can be seen that dodecanol shows some feature peaks locating at the wavenumbers of 3329, 2956, 2925, 2866 and 1467 cm^{-1}, which can be also found in the FTIR spectrum of Co_3O_4 QDs, demonstrating that the surface of newly synthesized Co_3O_4 QDs are really adsorbed by dodecanol. Nevertheless, after the coating process of EY on Co_3O_4 QDs, the feature peaks of dodecanol disappear. Instead, some new peaks similar to the feature peaks of Eosin Y are found, which indicates that dedacanol is removed, and only EY adsorbs on the surface of Co_3O_4 QDs in the Co_3O_4 QDs/EY sample, in accord with the description of EY sensitization process (see ESI).

Above all, the results of PXRD, XPS, TEM and FTIR jointly indicate

[a] International Research Center for Renewable Energy (IRCRE), State Key Laboratory of Multiphase Flow in Power Engineering (MFPE), Xi'an Jiaotong University (XJTU), 28 West Xianning Road, Xi'an, Shaanxi 710049, P. R. China. E-mail: lj-guo@mail.xjtu.edu.cn

†Electronic Supplementary Information (ESI) available: [The process of EY sensitization; PXRD spectra of Co_3O_4 QDs/EY and Co_3O_4 QDs; Survey scan XPS spectra and high-resolution XPS spectra in Co 2p of Co_3O_4 QDs/EY and Co_3O_4 QDs; TEM and HRTEM images of Co_3O_4 QDs and (b) Co_3O_4 QDs/EY; FTIR spectra of Eosin Y, Co_3O_4 QDs/EY, dodecanol and Co_3O_4 QDs.]. See DOI: 10.1039/x0xx00000x

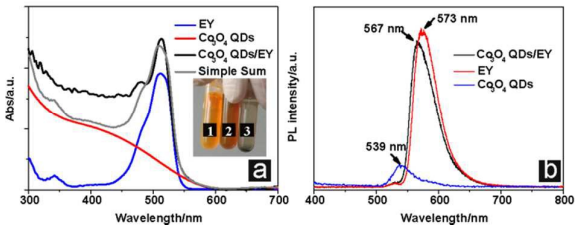

Fig.1 (a) UV-Vis diffusive reflectance and (b) photoluminescence spectra of EY, Co_3O_4 QDs and Co_3O_4 QDs/EY. Inset of (a): photographs of 1) EY, 2) Co_3O_4 QDs/EY and 3) Co_3O_4 QDs. Excitation wavelength of PL was 420 nm. Test conditions of (a) and (b): The concentration of TEOA and pH in each system were 0.29 M and 10.95, respectively. The weight concentration of Co_3O_4 QDs was 0.01 mg mL^{-1} in Co_3O_4 QDs/EY and Co_3O_4 QDs systems. The concentration of EY was 0.01 mM in Co_3O_4 QDs/EY and EY systems.

that, in the Co_3O_4 QDs/EY sample, EY just adsorbs on the surface of Co_3O_4 QDs, and has little effect on elemental and phase compositions, crystal structures, and particle morphologies of Co_3O_4 QDs.

UV-Vis diffusive reflectance, photoluminescence (PL) spectra and the PL decay curves were measured on three liquid samples. UV-Vis spectra (see Fig. 1a) show that the absorption edge of Co_3O_4 QDs solution locates at about 600 nm, while the absorption peak of EY solution centers at 518 nm. When Co_3O_4 QDs is added into the EY solution, the absorbance is different from the simple sum of Co_3O_4 QDs and EY, which implies that some interaction really exists between Co_3O_4 QDs and EY. Another evidence of interaction is presented in the insert picture of Fig. 1a. As it is shown, Co_3O_4 QDs can be dispersed in EY/TEOA solution easily and form a stable colloidal solution, while they are difficult to be disperse in absolute TEOA solution and precipitate rapidly. This result deduces that, due to the interaction between EY and Co_3O_4 QDs, EY is adsorbed on the surface of Co_3O_4 QDs and protects Co_3O_4 QDs from the effects of agglomeration and precipitation which are caused by TEOA. The interaction between EY and Co_3O_4 QDs is further supported by PL spectra (see Fig. 1b). It shows that the peak of Co_3O_4 QDs locates at 539 nm, while that of EY locates at 567 nm. Compared with that of EY, the PL peak of Co_3O_4 QDs/EY performs red-shift, which can be mainly ascribed to the noncovalent π–π interaction of Co_3O_4 QDs with EY and the interfacial electron transfers from the attached EY* to the Co_3O_4 QDs.[11,12] And this interaction benefits the transmission of charge between EY and Co_3O_4 QDs. The PL decay curves (see Fig. S6, ESI†) show that the fluorescence lifetime of EY is 0.303 ns, which changes insignificantly in the presence of Co_3O_4 QDs (0.319 ns). This result reveals that the exist of Co_3O_4 QDs has little effect on the fluorescence lifetime of system.

To further investigate the transmission capability of electrons from semiconductor surfaces to water, the linear sweep voltammetry (LSV) technique is employed. As shown in Fig. 2a, at the same applied bias, the value of cathodic current of Co_3O_4 QDs-FTO is higher than that of P25 TiO_2-FTO and FTO. This result reveals that electrons in Co_3O_4 QDs can easily transfer from semiconductor surfaces to water for H^+ reduction and H_2 production.[13] Transient photocurrent–time profiles of Co_3O_4 QDs-FTO is inserted in Fig. 2a, which shows that the current value of Co_3O_4 QDs-FTO increases in negative direction under light irradiation. And this result conforms that Co_3O_4 QDs is a p-type semiconductor. To investigate the structure of energy band on the surface of Co_3O_4 QDs, Mott-Schottky plots and open circuit potential-time (OCPT) curve were measured on a Co_3O_4 QDs-FTO electrode. As shown in Fig. 2b, the flat band potential (E_{FB}) of Co_3O_4 QDs, which can be determined by the x-axis intercept of straight-line portion of Mott-Schottky plots (dark), is 0.67 V vs. Ag/AgCl. And the open circuit potential (E_{OCP}) is 0.42 V vs. Ag/AgCl, which is lower than the flat band potential. This results suggest that energy bands bend downwards on the surface of Co_3O_4 QDs if Fermi level pins. However, according to literature[14], the adsorption of organic molecules can form surface states which will trap minority carriers and cause Fermi level unpinning under light irradiation. To evaluate the effect of surface states, Mott-Schottky plot under visible-light (λ ≥ 420 nm) irradiation was measured. It can be seen that the x-axis intercept of straight-line portion of Mott-Schottky plot (illumination) shifts only 0.01 V cathodically compared with that of Mott-Schottky plot (dark). This result indicates that surface states have little effect on the structure of energy band, and thus the energy bands of Co_3O_4 QDs performs downwards bending.

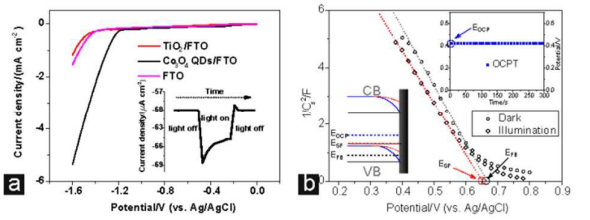

Fig.2 (a) LSV curves of bare FTO glass and Co_3O_4 QDs- and P25 TiO_2-coated FTO electrodes in a solution of 0.1 mol/L Na_2SO_4 at pH 7. The scan rate was 1 mV s^{-1}. Insert of (a): Transient photocurrent–time profiles of Co_3O_4 QDs-FTO with applied bias of -0.2V (vs Ag/AgCl). (b) Mott-Schottky plots and open circuit potential-time (OCPT) curve of a Co_3O_4 QDs-FTO electrode. Test conditions of (b): pH and the concentration of TEOA and EY were 10.95, 0.29 M and 40 mM, respectively.

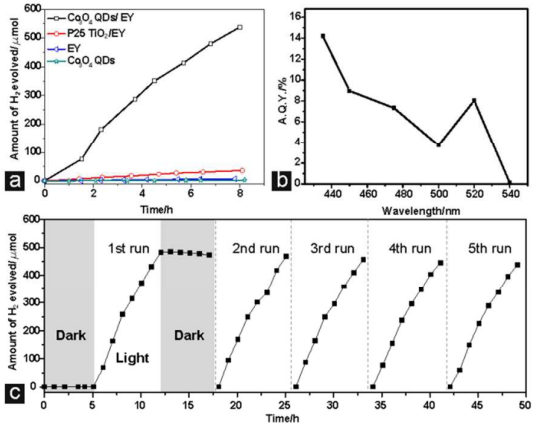

Fig.3 (a) Time courses of hydrogen evolution over Co_3O_4 QDs/EY, P25 TiO_2/EY, EY and Co_3O_4 QDs systems. (b) The action spectrum of Co_3O_4 QDs/EY system . The system was irradiated with a 300 W Xe lamp with a bandpass filter. The testing time was 2 h. (c) Stability testing of H_2 evolution over Co_3O_4 QDs/EY system. The reaction was continued for 5 runs (~7 h each run). Before each run, some TEOA was added into system to keep pH 10.95. Test conditions of (a), (b) and (c): The concentration of TEOA and pH in each system were 0.29 M and 10.95, respectively. The weight concentration of photocatalysts was 50 mg L^{-1} in P25 TiO_2/EY, Co_3O_4 QDs/EY and Co_3O_4 QDs systems. The concentration of EY was 40 mM in Co_3O_4 QDs/EY, P25 TiO_2/EY and EY systems.

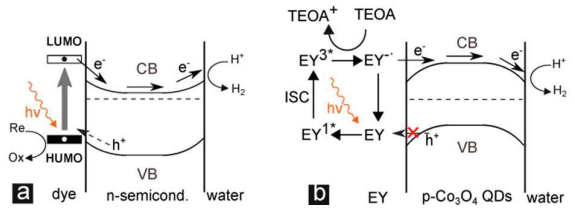

Fig.4 Simplified scheme of energy band bending and charge transmission in (a) dye-sensitized n-type semiconductor system and (b) EY-sensitized p-type Co_3O_4 QDs system.

Fig. 3a shows the photocatalytic activities for H_2 evolution over EY, Co_3O_4 QDs, Co_3O_4 QDs/EY and P25 TiO_2/EY under visible-light ($\lambda \geq 420$nm) irradiation in 100 mL aqueous TEOA solution. In order to reduce the mechano-catalytic H_2 production effect,[15] the photocatalytic systems was run with weakly stirring. Control experiments showed that no H_2 was formed when the reaction proceeded in TEOA aqueous solution without Co_3O_4 QDs/EY, pure water or in the dark while other conditions remained unchanged. As shown in Fig. 3a, in absence of EY or Co_3O_4 QDs, the system of Co_3O_4 QDs/EY performs almost no H_2 produced for 7 h, which indicates that the photocatalytic efficiency of single Co_3O_4 QDs is very low and the electron generated on the excited EY can not transfer to solution for H^+ reduction easily without semiconductor photocatalysts. The system of P25 TiO_2/EY also shows low H_2 production rate, about 4.4 μmol h^{-1},which is consistent with the reported work[16]. This result implies that, due to high over-potential, electrons in the conduction band of TiO_2 which are transferred from EY can not reduce H^+ effectively without cocatalysts. However, the Co_3O_4 QDs/EY system shows higher photocatalytic activity than that of P25 TiO_2/EY, and the rate of H_2 evolved is 67.2 μmol h^{-1} (~13440 μmol h^{-1} g^{-1}_{cat}) in 7 h, which is 15.3 times higher than that of the latter at the same experimental conditions. As far as we know, this value can be one of the highest value in the systems of EY-sensitized oxide semiconductor for H_2 production without loading cocatalyst under visible light irradiation. To investigate the wavelength dependence of photocatalytic H_2 evolution, the action spectrum of Co_3O_4 QDs/EY systems was examined over a wide visible light range of 435−540 nm (see Fig. 3b). As shown in Fig. 3b, the apparent quantum yield (A.Q.Y.) of the system shows the trend of rising-declining-rising with the decrease of the incident wavelength. A locally maximal A.Q.Y. located at 520 nm is 8.1% due to strong absorption of light of EY, and the globally maximal A.Q.Y. located at 435 nm is 14.2% due to higher energy of photons. The conversion efficiency of solar energy to hydrogen energy on Co_3O_4 QDs/EY systems at room temperature and under 100 mW/cm illumination in a solar simulator with an AM1.5 global filter is 1.37%.

Furthermore, the stability of the Co_3O_4 QDs/EY system for 5 runs (~7 hours each run) were carried out under visible light ($\lambda \geq 420$nm) irradiation(see Fig. 3c). In the first run, the controlling experiments were carried out in dark before and after photocatalytic reaction, which shows that the system performs no photocatalytic activity without light irradiation. The average rates of hydrogen evolution of first, second, third, fourth and fifth run are 67.2, 66.8, 65.2, 63.6 and 62.4 μmol h^{-1}. No significant decrease of H_2 evolution is observed after 5 runs, indicating the good stability of the present system for photocatalytic H_2 production.

The high and stable photocatalytic activity of EY-sensitized p-type Co_3O_4 QDs for water reduction and hydrogen production under visible-light irradiation without any cocatalyst can be explained by the theory of energy band bending induced by space charge region. When dye adsorbs on the surface of semiconductor, the free electrons/holes will transfer between dye and semiconductor due to the existence of interaction and the chemical potential difference. This transmission of electrons/holes causes the free charge carrier concentration near the semiconductor surface to be different from the bulk, thus forms the known space charge region.[17] In the space charge region, energy band of semiconductor performs bending due to the electric field.[17-20] Similarly, near the surface of semiconductor and water, energy band bending is also formed.[20] In a tranditional dye-sensitized semiconductor system, n-type semiconductor, such as TiO_2, is usually used as catalyst. As it is shown in Fig. 4a, on the surface between n-type semiconductor and dye, the energy bands of n-type semiconductor bend upward, and the electron can flow from excited dye molecule to the conduction band (CB) of n-type semiconductor. However, the upward bent bands on the surface between n-type semiconductor and water increase the barrier width and height for electron tunneling from the CB of the semiconductor to water, decreasing the electron transmission probability from semiconductor to water for reduction reaction. Thus dye-sensitized n-type semiconductor system performs low photocatalytic activity without cocatalyst. In the EY-sensitized p-type Co_3O_4 QDs system, as it is shown in Fig. 4b, the downward bent bands on the surface between Co_3O_4 QDs and EY forms a barrier which hinders electron transmission from EY molecule to the conduction band (CB) of p-type Co_3O_4 QDs. Under visible light irradiation, EY will gain a photon and produce singlet excited state EY^{1*}, and subsequently produce a lowest-lying triplet excited state EY^{3*} which owns a long life time via an intersystem crossing (ISC). EY^{3*} will be reductively quenched by a sacrificial donor TEOA to produce $EY^{-\bullet}$.[12] Because the free electron in $EY^{-\bullet}$ species has a much higher chemical potential than that in the CB of Co_3O_4 QDs, it tend to jump over the barrier and flow to the CB of Co_3O_4 QDs. After losing electron, $EY^{-\bullet}$ changes back to EY, and the electron cannot transfer from the CB of p-type Co_3O_4 QDs to EY again. On a surface between p-type Co_3O_4 QDs and water, the energy bands bend downward, and the tunneling barrier is eliminated, which facilitates the electron transfer across the surface of Co_3O_4 QDs to water for reduction reaction. Thus EY-sensitized p-type Co_3O_4 QDs performs high photocatalytic activity for water reduction and hydrogen production under visible-light irradiation without any cocatalyst. Moreover, the barrier on the surface between Co_3O_4 QDs and EY can prevent the transport of photo- or thermal-excited holes from the valance band of p-type Co_3O_4 QDs to EY molecule, thus reduces oxidative damage of EY and further enhances the stability of the system.

Conclusions

In summary, we present a cocatalyst-free, highly efficient and stable EY-sensitized p-type Co_3O_4 QDs system for visible-light-driven H_2 production. The system exhibits an average hydrogen evolution rate of 67.2 μmol h^{-1} (~13440 μmol h^{-1} g^{-1}, $\lambda \geqslant 420$ nm). This high and stable photocatalytic activity is

mainly due to energy band bending: 1) on the surface between p-type Co_3O_4 QDs and water, the downward bent bands facilitates the electron transfer across the surface of Co_3O_4 QDs to water; 2) on the surface between p-type Co_3O_4 QDs and EY, the downward bent bands prevent holes transmission from the valance band of p-type Co_3O_4 QDs to EY molecule, which reduces oxidative damage of EY and further enhances the stability of the system. This work provides a promising strategy for designing efficient and stable photocatalytic hydrogen generation systems based on p-type semiconductor.

Acknowledgements

We are grateful for financial support by the National Natural Science Foundation of China (Nos. 51236007 and 51323011), the China Postdoctoral Science Foundation (Nos.2014T70915), the Natural Science Basic Research Plan in Shaanxi Province of China (No.2014JQ2-5022), and the Postdoctoral Science Foundation in Shaanxi Province of China.

Notes and references

1 W. J. Youngblood; S-H. A. Lee; K. Maeda; T. E. Mallouk, *Acc. Chem. Res.*, 2009, **42**, 1966−1973.
2 W. Zhang; J. D. Hong; J. W. Zheng; Z. Y. Huang; J. R. Zhou; R. Xu, *J. Am. Chem. Soc.*, 2011, **133**, 20680−20683.
3 J. W. Shi; X. Guan; Z. Zhou; H. Liu; L. J. Guo, *J. Nanopart. Res.,* 2015, **17**, 252.
4 P. W. Du; R. Eisenberg, *Energy Environ. Sci.*, 2012, **5**, 6012−6021.
5 M. G. Walter; E. L. Warren; J. R. McKone; S. W. Boettcher; Q. Mi; E. A. Santori; N. S. Lewis, *Chem. Rev.*, 2010, 110, 6446−6473.
6 N. Z. Bao; L. M. Shen; T. Takata; K. Domen, *Chem. Mater.*, 2008, **20**, 110−117.
7 H. Yan; J. Yang; G. Ma; G. Wu; X. Zong; Z. Lei; J. Shi; C. Li, *J. Catal.*, 2009, **266**, 165−168.
8 N. Zhang; J. Shi; S. S. Mao; L. Guo, *Chem. Commun.*, 2014, **50**, 2002-2004.
9 L. Fu; Z. M. Liu; Y. Q. Liu; B. X. Han; P. G. Hu; L. C. Cao; D. B. Zhu, *Adv. Mater.*, 2005, **17**, 217-221.
10 J. Li; W. Zhao; F. Huang; A. Manivannan; N. Wu, *Nanoscale*., 2011, **3**, 5103-5109
11 H. Zhang; X. Lv; Y. Li; Y. Wang; J. Li, *ACS Nano*, 2010, **4**, 380−386
12 C. Kong; S. Min; G. Lu, *ACS Catal*., 2014, **4**, 2763-2769.
13 X. Zong; G. P. Wu,; H. J. Yan; G. J. Ma; J. Y. Shi; F. Y. Wen; L. Wang; C. Li, *J. Phys. Chem. C*, 2010, **114**, 1963−1968.
14 A. Hagfeldt; U. Bjorksten; M. Gratzel, *J. Phys. Chem.*, 1996, **100**, 8045-8048.
15 S. Ikeda; T. Takata; T. Kondo; G. Hitoki; M. Hara; J. N. Kondo; K. Domen; H. Hosono; H. Kawazoe; A. Tanaka, *Chem. Commun.*, 1998, **998**, 2185-2186.
16 Z. Yan; X. Yu; Y. Zhang; H. Jia; Z. Sun; P. Du, *Appl. Catal. B-Environ.*, 2014, **160**, 173-178.
17 Z. Zhang; J. T. Yates, *Chem. Rev.*, 2012, **112**, 5520−5551
18 L Li; P. A. Salvadora; G. S. Rohrer, *Nanoscale,* 2014*,* **6***,* 24-42.
19 C. Yang; Q. Zhu; T. Lei; H. Lia; C. Xie, *J. Mater. Chem. C*, 2014, **2**, 9467-9477.
20 M. G. Walter; E. L. Warren; J. R. McKone; S. W. Boettcher; Q. Mi; E. A. Santori; N. S. Lewis, *Chem. Rev.*, 2010, **110**, 6446–6473.